

# Dual Function of Antireflectance and Surface Passivation of Atomic-Layer-Deposited Al<sub>2</sub>O<sub>3</sub> Films

Li Qiang Zhu, Xiang Li, Zhong Hui Yan, Hong Liang Zhang, and Qing Wan

**Abstract**—Surface antireflectance and passivation properties of the Al<sub>2</sub>O<sub>3</sub> films deposited on Czochralski Si wafers by atomic layer deposition (ALD) are investigated. Textured Si with 100-nm Al<sub>2</sub>O<sub>3</sub> shows a very low average reflectance of  $\sim 2.8\%$ . Both p- and n-type Si wafers are well passivated by Al<sub>2</sub>O<sub>3</sub> films. The maximal minority carrier lifetimes are improved from  $\sim 10 \mu\text{s}$  before Al<sub>2</sub>O<sub>3</sub> passivation to above 3 ms for both p- and n-type Si after Al<sub>2</sub>O<sub>3</sub> film deposition and annealing at an appropriate temperature. Hence, an ALD-deposited Al<sub>2</sub>O<sub>3</sub> film shows the dual function of antireflectance and surface passivation for solar cell applications.

**Index Terms**—Antireflectance, atomic layer deposition (ALD)-deposited Al<sub>2</sub>O<sub>3</sub> film, Si solar cells, surface passivation.

## I. INTRODUCTION

Al<sub>2</sub>O<sub>3</sub> thin films provide excellent surface passivation on both lightly and highly doped p- and n-type crystalline silicon (c-Si) surfaces, resulting in the improved efficiency [1]–[5], which is attributed to a low density of interface defects  $D_{it}$  in the range of  $10^{11} \text{ cm}^{-2} \cdot \text{eV}^{-1}$  and a field-effect passivation with a high density of fixed negative charges  $Q_{fix}$  above  $10^{12} \text{ cm}^{-2}$  [1], [6]. To activate the passivation, an annealing step at moderate temperatures after deposition was reported to be essential [7]. At the same time, effective antireflectance plays an important role for solar cells efficiency improvement. Conventionally, the textured Si surface coated with a SiN<sub>x</sub> antireflective layer from the production line shows an average reflectance of below 5%. Although the strong passivation performance for Al<sub>2</sub>O<sub>3</sub> films have been reported, the antireflective properties of Al<sub>2</sub>O<sub>3</sub> films have not been reported yet [1]–[7]. In this letter, both antireflectance properties and passivation properties of the Al<sub>2</sub>O<sub>3</sub> films deposited by atomic layer deposition (ALD) are studied. A minimal reflectance of  $\sim 2.8\%$  is obtained. A maximal minority carrier lifetime of above 3 ms was obtained for both p- and n-type Si passivated by Al<sub>2</sub>O<sub>3</sub>. Such results indicate that Al<sub>2</sub>O<sub>3</sub> films have the dual function of antireflectance and surface passivation, which is favorable for c-Si solar cell applications.

Manuscript received August 23, 2012; revised September 10, 2012; accepted September 13, 2012. Date of publication October 26, 2012; date of current version November 22, 2012. This work was supported in part by the National Natural Science Foundation of China under Grant 11104288 and in part by the Ningbo Natural Science Foundation under Grant 2011A610202. The review of this letter was arranged by Editor S. J. Koester.

The authors are with the Ningbo Institute of Materials Technology and Engineering, Chinese Academy of Sciences, Ningbo 315201, China (e-mail: wanqing@nimte.ac.cn).

Digital Object Identifier 10.1109/LED.2012.2219491

## II. EXPERIMENTAL DETAIL

The 400- $\mu\text{m}$ -thick (100)-oriented p-type ( $\rho = 30 \Omega \cdot \text{cm}$ ) and n-type ( $\rho = 5.5 \Omega \cdot \text{cm}$ ) Czochralski (CZ) Si wafers were used as the substrates. For antireflectance investigation, some Si wafers were textured by  $\sim 1.2\%$  NaOH solution at  $\sim 80^\circ\text{C}$  for  $\sim 20$  min. All substrates underwent an HCl solution dip for 5 min followed by a dilute HF dip. A deionized water rinse was adopted after each chemical dip step. Al<sub>2</sub>O<sub>3</sub> films with different thicknesses were deposited on both sides of the Si wafers to obtain symmetric lifetime samples by a thermal NCD 200B ALD reactor at  $200^\circ\text{C}$  with a 100-sccm background flow of N<sub>2</sub>. A cycle in the reactor consisted of a 0.3-s injection of Al(CH<sub>3</sub>)<sub>3</sub> vapors followed by 7-s N<sub>2</sub> purge and a 0.1-s injection of H<sub>2</sub>O vapor followed by 7-s N<sub>2</sub> purge, resulting in a deposition rate of 1.25 Å/cycle. The lifetime samples were annealed at different temperatures in atmosphere ambient. SiN<sub>x</sub> was deposited by plasma-enhanced chemical vapor deposition on the same textured Si at the production line for antireflectance comparison, which is noted as the standard (STD SiN<sub>x</sub>) sample.

X-ray photoelectron spectroscopy and scanning electron microscopy (SEM) are used for structural characterization. Spectroscopic ellipsometry has been employed to investigate the optical characteristics and the thickness of Al<sub>2</sub>O<sub>3</sub> films on shiny-etched Si with the incidence angle of  $55^\circ$ ,  $65^\circ$ , and  $75^\circ$ . The reflectance spectrum was measured by an AudioDev Helios LAB-rc system. Reflected light from a broadband halogen light source is collected and detected by a special designed integrating sphere. The average reflectance was calculated between 380 and 1090 nm, without any weighting. Effective minority carrier lifetime  $\tau_{eff}$  is measured after annealing on a Semilab WT-2000PVN lifetime tester. The maximum achieved  $\tau_{eff}$  were investigated. Lifetime  $\tau_{eff}$  depends on both bulk minority carrier lifetime  $\tau_{bulk}$  and surface recombination velocity  $S_{eff}$  [8], i.e.,

$$\frac{1}{\tau_{eff}} = \frac{1}{\tau_{bulk}} + \frac{2S_{eff}}{W} \quad (1)$$

where  $W$  is the wafer thickness. The bulk minority carrier lifetime was assumed to be infinite. Accordingly, the calculated  $S_{eff}$  value marks an upper limit to the effective surface recombination velocity.

## III. RESULTS AND DISCUSSION

An SEM image of the textured Si surface shows typical pyramid structures. The thicknesses of Al<sub>2</sub>O<sub>3</sub> films are determined to be  $\sim 100$ ,  $\sim 70$ , and  $\sim 30$  nm for 800, 560, and 240 ALD cycles, respectively. X-ray photoelectron spectroscopy results indicate that Al<sub>2</sub>O<sub>3</sub> is stoichiometric with an O/Al ratio

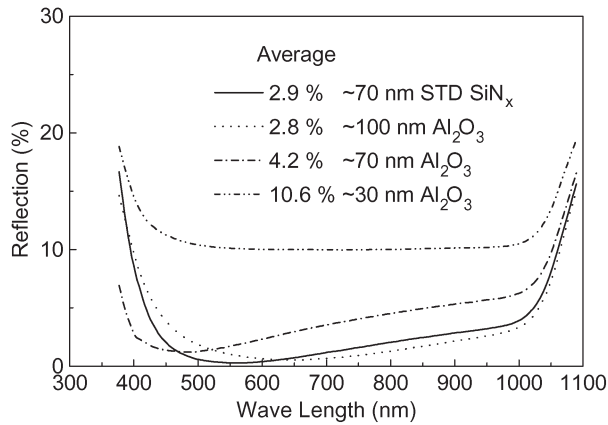


Fig. 1. Reflectance curves for the  $\text{Al}_2\text{O}_3$ -coated textured Si. Results for the standard  $\text{SiN}_x$ -coated textured Si (STD  $\text{SiN}_x$ ) are included for comparison.

of  $\sim 1.53$ . The refractive index is measured to be  $\sim 1.65$  at a wavelength of 630 nm, which is similar to the reported value [9]. Optical band gap  $E_g$  is extracted to be  $\sim 6$  eV, which means that the deposited  $\text{Al}_2\text{O}_3$  layer is transparent for the wavelength above 200 nm. The obtained results are meaningful for antireflectance applications in solar cells.

Fig. 1 shows the reflectance spectrum of the  $\text{Al}_2\text{O}_3$ -coated textured Si wafers with different film thicknesses. The reflectance for the STD  $\text{SiN}_x$  sample is also included for comparison. The average reflectance is  $\sim 10.6\%$  and  $\sim 4.2\%$  when depositing  $\sim 30$ -nm  $\text{Al}_2\text{O}_3$  and  $\sim 70$ -nm  $\text{Al}_2\text{O}_3$  on textured Si, respectively. Meaningfully, the reflectance spectra for  $\sim 100$ -nm  $\text{Al}_2\text{O}_3$ -coated textured Si are quite similar to that of the STD sample. At shorter wavelength, the reflectance for  $\sim 100$ -nm  $\text{Al}_2\text{O}_3$  is slightly higher than the STD sample, whereas at longer wavelength, the reflectance is slightly lower than the STD sample, which results in the best reflectance of  $\sim 2.8\%$  for  $\sim 100$ -nm  $\text{Al}_2\text{O}_3$  on the textured Si, close to  $2.9\%$  for the STD  $\text{SiN}_x$  sample. Such differences may be due to the different refractive index between  $\text{SiN}_x$  and  $\text{Al}_2\text{O}_3$ . The aforementioned results indicate the potential antireflectance applications of  $\text{Al}_2\text{O}_3$  in c-Si solar cells.

A low lifetime of  $\sim 6.0$   $\mu\text{s}$  is obtained for the original p-Si wafer. After a 100-nm-thick  $\text{Al}_2\text{O}_3$  deposition, a moderate surface passivation level with effective minority carrier lifetimes  $\tau_{\text{eff}}$  of  $\sim 140$   $\mu\text{s}$  is obtained, which is similar to that observed for conventional thermal ALD [10]. Similarly, a 30-nm-thick  $\text{Al}_2\text{O}_3$  deposition results in higher effective minority carrier lifetimes  $\tau_{\text{eff}}$  of  $\sim 910$   $\mu\text{s}$ . To study the full potential for the surface passivation and the thermal stability of the  $\text{Al}_2\text{O}_3$  layers, the lifetime samples were exposed to postdeposition annealing in atmosphere ambient for 5 min with temperature ranging from 300  $^\circ\text{C}$  to 650  $^\circ\text{C}$ . Fig. 2(a) illustrates the effective minority carrier lifetime of  $\text{Al}_2\text{O}_3$ -passivated p-type Si wafers as a function of the applied thermal treatment temperature. Flash annealing was also performed at 900  $^\circ\text{C}$  for 3 s. For the 100-nm  $\text{Al}_2\text{O}_3$ -coated samples, annealing performed at 600  $^\circ\text{C}$  for 5 min yields a good passivation with a lifetime of  $\sim 750$   $\mu\text{s}$ . While for the 30-nm  $\text{Al}_2\text{O}_3$ -coated samples, the best passivation is obtained at 350  $^\circ\text{C}$  with a lifetime of  $\sim 4.7$  ms. Annealing at higher temperature results in the deteriorated lifetime. The flash annealing at 900  $^\circ\text{C}$  for 3 s for the 30-nm  $\text{Al}_2\text{O}_3$ -coated lifetime samples yields a moderate level of surface passivation with a lifetime

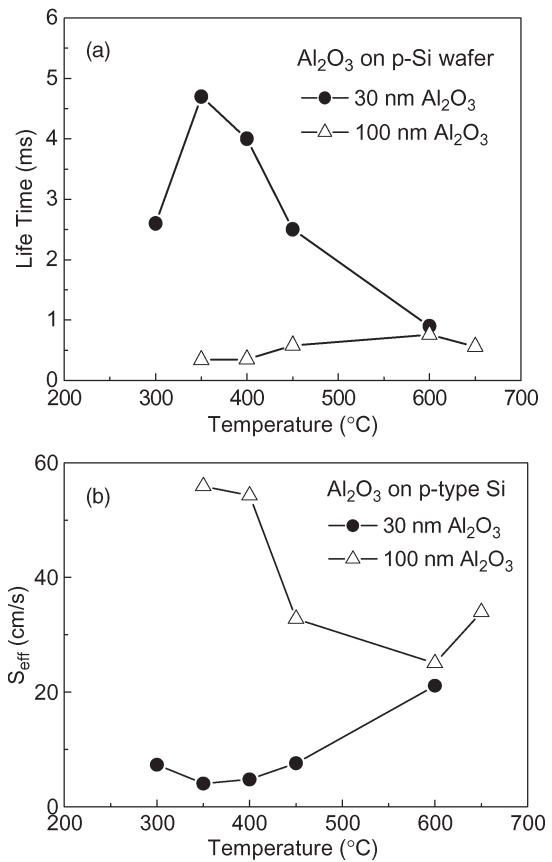


Fig. 2. (a) Lifetime values for p-type Si passivated by 100- and 30-nm  $\text{Al}_2\text{O}_3$ . (b) Effective surface recombination velocity  $S_{\text{eff}}$ .

of 120  $\mu\text{s}$ . The passivation stabilities have been studied for the annealed samples. After two months in air ambient, the lifetime is reduced from 4.7, 4, and 2.5 ms to 2.5, 2.4, and 1.5 ms, for 350  $^\circ\text{C}$ , 400  $^\circ\text{C}$ , and 450  $^\circ\text{C}$  annealed 30-nm  $\text{Al}_2\text{O}_3$ -passivated p-type Si, respectively. Such degradations might be due to the decreased negative charge densities.

The upper limit of the effective surface recombination velocity was also calculated. For the original Si wafer, a high  $S_{\text{eff}}$  value of  $\sim 3200$  cm/s is determined. Before annealing, the 100-nm  $\text{Al}_2\text{O}_3$ -passivated p-type Si wafer shows a moderate  $S_{\text{eff}}$  of  $\sim 130$  cm/s, whereas the 30-nm  $\text{Al}_2\text{O}_3$ -passivated p-type Si wafer shows a lower  $S_{\text{eff}}$  of  $\sim 20$  cm/s. The postdeposition annealing treatment results in the improved  $S_{\text{eff}}$  [as shown in Fig. 2(b)]. For 100-nm  $\text{Al}_2\text{O}_3$ -coated Si wafers, the best results are obtained at 600  $^\circ\text{C}$ , yielding the lowest  $S_{\text{eff}}$  of  $\sim 25$  cm/s. While for 30-nm  $\text{Al}_2\text{O}_3$ -coated Si wafers, a very low  $S_{\text{eff}} < 20$  cm/s is obtained. The lowest  $S_{\text{eff}}$  of  $\sim 4$  cm/s is addressed at 350  $^\circ\text{C}$ . The flash annealing at 900  $^\circ\text{C}$  for 3 s yields a moderate level of surface passivation with an  $S_{\text{eff}}$  of  $\sim 160$  cm/s.

Capacitance–voltage (1.0 MHz) characterizations were measured by a Keithley 4200 SCS semiconductor parameter analyzer on MOS structures with  $\text{Al}_2\text{O}_3$  films with different thicknesses, as shown in Fig. 3. High densities of negative fixed charges are obtained for both the 30- and 100-nm  $\text{Al}_2\text{O}_3$  on the order of  $\sim 10^{12}$ /cm $^2$  by using the following relation:  $V_{\text{fb}} = \Phi_{\text{ms}} - Q_{\text{fix}}T_{\text{Al}_2\text{O}_3}/\epsilon_{\text{Al}_2\text{O}_3}$ . The high densities of the negative fixed charges in the 30-nm films result in a strong field-effect passivation [6]. A big stretch-out in the  $C$ – $V$  curves for the

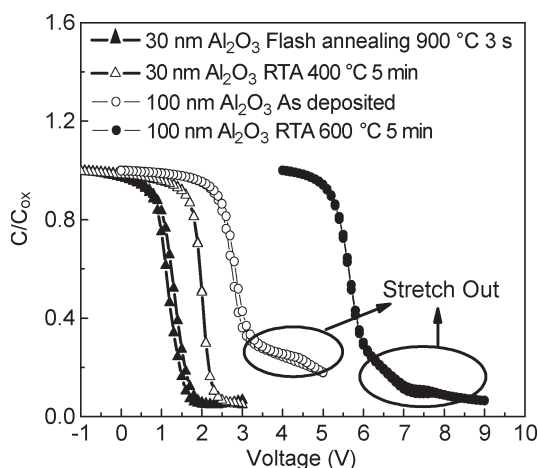


Fig. 3. Normalized  $C-V$  curves of MOS structures with  $\text{Al}_2\text{O}_3$  films on p-type Si substrates measured at 1.0 MHz.

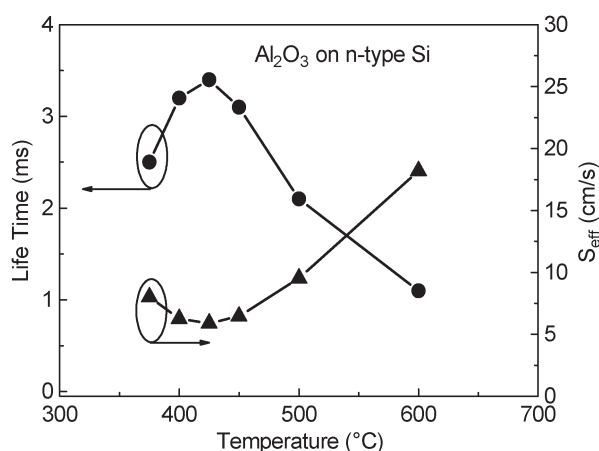


Fig. 4. Lifetime values for n-type Si passivated by 100-nm  $\text{Al}_2\text{O}_3$  and the effective surface recombination velocity  $S_{\text{eff}}$ .

100-nm  $\text{Al}_2\text{O}_3$  is observed, which is likely due to the high-density interfacial state  $D_{\text{it}}$  and defects. Hence, the 100-nm  $\text{Al}_2\text{O}_3$  shows a relatively poorer passivation performance.

Similarly, n-type Si wafers are also passivated by 100-nm-thick  $\text{Al}_2\text{O}_3$ , as shown in Fig. 4. The original n-type Si wafer shows a low minority carrier lifetime of  $\sim 13 \mu\text{s}$ . After passivated with 100-nm-thick  $\text{Al}_2\text{O}_3$ , the effective minority carrier lifetime increased to 1.2 and 3.4 ms for the as-deposited sample and the  $425^\circ\text{C}$  annealed sample, respectively. The flash annealing at  $900^\circ\text{C}$  for 3 s yields a moderate level of surface passivation with a lifetime of  $450 \mu\text{s}$ . The upper limit of the effective surface recombination velocity is obtained. The n-type Si wafer passivated by a 100-nm  $\text{Al}_2\text{O}_3$  layer shows a low  $S_{\text{eff}}$  of  $\sim 16 \text{ cm/s}$  before annealing. The lowest  $S_{\text{eff}}$  of  $\sim 6 \text{ cm/s}$

is obtained after annealing at  $425^\circ\text{C}$ . The flash annealing at  $900^\circ\text{C}$  for 3 s yields a moderate level of surface passivation with an  $S_{\text{eff}}$  of  $44 \text{ cm/s}$ .

#### IV. CONCLUSION

In summary,  $\text{Al}_2\text{O}_3$  layers have been deposited by thermal ALD on both p- and n-type CZ Si wafers. The textured Si coated with 100-nm  $\text{Al}_2\text{O}_3$  shows a low average reflectance of  $\sim 2.8\%$ . Both p- and n-type Si wafers can be well passivated by  $\text{Al}_2\text{O}_3$  films. The maximal minority carrier lifetimes are improved from  $\sim 10 \mu\text{s}$  to above 3.0 ms for both p- and n-type Si after  $\text{Al}_2\text{O}_3$  passivation and annealing. Hence, the dual function of antireflectance and surface passivation of an ALD-deposited  $\text{Al}_2\text{O}_3$  film was demonstrated, which has potential application in c-Si solar cells.

#### REFERENCES

- [1] F. Werner, B. Veith, V. Tiba, P. Poedt, F. Roozeboom, R. Brendel, and J. Schmidt, "Very low surface recombination velocities on p- and n-type c-Si by ultrafast spatial atomic layer deposition of aluminum oxide," *Appl. Phys. Lett.*, vol. 97, no. 16, pp. 162103-1–162103-3, Oct. 2010.
- [2] N. M. Terlinden, G. Dingemans, M. C. M. Van de Sanden, and W. M. M. Kessels, "Role of field-effect on c-Si surface passivation by ultrathin (2–20 nm) atomic layer deposited  $\text{Al}_2\text{O}_3$ ," *Appl. Phys. Lett.*, vol. 96, no. 11, pp. 112101-1–112101-3, Mar. 2010.
- [3] B. Hoex, M. C. M. Van de Sanden, J. Schmidt, R. Brendel, and W. M. M. Kessel, "Surface passivation of phosphorus-diffused  $n^+$ -type emitters by plasma-assisted atomic-layer deposited  $\text{Al}_2\text{O}_3$ ," *Phys. Stat. Sol. RRL*, vol. 6, no. 1, pp. 4–6, Jan. 2012.
- [4] B. Vermang, H. Goverde, L. Tous, A. Lorenz, P. Choulant, J. Horzel, J. John, J. Poortmans, and R. Mertens, "Approach for  $\text{Al}_2\text{O}_3$  rear surface passivation of industrial p-type Si PERC above 19%," *Prog. Photovolt: Res. Appl.*, vol. 20, no. 3, pp. 269–273, May 2012.
- [5] H. Lee, T. Tachibana, N. Ikeno, H. Hashiguchi, K. Arafune, H. Yoshida, S.-I. Sato, T. Chikyow, and A. Ogura, "Interface engineering for the passivation of c-Si with  $\text{O}_3$ -based atomic layer deposited  $\text{Al}_2\text{O}_3$  for solar cell application," *Appl. Phys. Lett.*, vol. 100, no. 14, pp. 143901-1–143901-4, Apr. 2012.
- [6] B. Hoex, J. J. H. Gielis, M. C. M. Van de Sanden, and W. M. M. Kessels, "On the c-Si surface passivation mechanism by the negative-charge-dielectric  $\text{Al}_2\text{O}_3$ ," *J. Appl. Phys.*, vol. 104, no. 11, pp. 113 703-1–113 703-7, Dec. 2008.
- [7] J. Benick, A. Richter, T. T. A. Li, N. E. Grant, K. R. McIntosh, Y. Ren, K. J. Weber, M. Hermle, and S. W. Glunz, "Effect of a post-deposition anneal on  $\text{Al}_2\text{O}_3/\text{Si}$  interface properties," in *Proc. 35th IEEE Photovolt. Spec. Conf.*, Honolulu, HI, 2010, pp. 000891–000896.
- [8] B. Hoex, J. Schmidt, P. Pohl, M. C. M. Van de Sanden, and W. M. M. Kessels, "Silicon surface passivation by atomic layer deposited  $\text{Al}_2\text{O}_3$ ," *J. Appl. Phys.*, vol. 104, no. 4, pp. 044903-1–044903-12, Aug. 2008.
- [9] P. Saint-Cast, D. Kania, M. Hofmann, J. Benick, J. Rentsch, and R. Preu, "Very low surface recombination velocity on p-type c-Si by high-rate plasma-deposited aluminum oxide," *Appl. Phys. Lett.*, vol. 95, no. 15, pp. 151502-1–151502-3, Oct. 2009.
- [10] G. Dingemans, R. Seguin, P. Engelhart, M. C. M. van de Sanden, and W. M. M. Kessels, "Silicon surface passivation by ultrathin  $\text{Al}_2\text{O}_3$  films synthesized by thermal and plasma atomic layer deposition," *Phys. Stat. Sol. RRL*, vol. 4, no. 1/2, pp. 10–12, Feb. 2010.